Software Tool for Wind Design of Cable Stayed Bridges

Authors:

Dorian Janjic, Dorian.Janjic@bentley.com
Johann Stampler, Johann.Stampler@bentley.com
Andreas Domaingo, Andreas.Domaingo@bentley.com
All: TDV Technische Datenverarbeitung Dorian Janjic & Partner GmbH/Bentley Systems, Gleisdorfer Gasse 5, 8010 Graz, Austria, office@tdv.at

INTRODUCTION

Although wind related phenomena on bridges have been observed since the 19th century and sometimes quite impressive as 1940 with the collapse of the first Tacoma Narrows bridge, comprehensive wind design is still on its way to a standard tool in bridge design. Because of its complexity it is only partly covered in design codes. There are good text books discussing the topic [Simiu and Scanlan, 1996, Strømmen, 2006], and the implementation of the methods therein can reduce design effort a great deal.

The first step for the treatment of wind effects is the characterization of the air flow around the involved cross sections in the form of several coefficients for steady state and fluctuating forces. Nowadays they are obtained in the majority by extensive wind tunnel tests. This is a complicated task, since a lot of similarity parameters must be considered. According to Simiu [1996], "the wind tunnel modeler is thus launched upon a series of inevitable compromises that render his task complex, revealing it as an art of both performance and interpretation rather than an exact science."

Since the 1990ies, the field of Computational Fluid Dynamics (CFD) is becoming an topic of interest in bridge engineering. Especially the field of vortex methods has gained great attention [Walther, 1994]. With suitable computational models, time traces of forces can be computed, which yield the desired aerodynamic coefficients in a post-processing step.

A detailed statistical characterization of the local wind properties is necessary to describe the buffeting response of a bridge adequately. To this end wind measurements are carried out to derive models for mean wind, turbulence intensity, power spectral density and wind coherence. This information is then used together with the aerodynamic coefficients in the framework of a modal analysis to estimate corresponding peak response of the bridge.

Quite different critical aero-elastic phenomena have been observed on existing bridges, and solving all these problems within one software package considerably eases the design process. These phenomena include across-wind galloping and wake galloping, torsional divergence and flutter phenomena. The susceptibility of the considered bridge deck to these phenomena can be investigated by applying several wind design checks, which will be outlined.

The present paper describes how the steps of computational modeling are implemented into one software package. Different application examples are outlined for the different analysis types. The investigation of steady state coefficients and related buffeting analysis is demonstrated for the Stonecutters bridge. Aspects of the flutter analysis are explained by considering the main deck cross section of the Great Belt East bridge.

DISCRETE VORTEX METHOD

A general description of air the spatial and temporal evolution of a fluid around a body is provided by the Navier-Stokes equations. For bluff body aerodynamics, like the cross sections considered in bridge engineering, it is common to consider the air as fluid with constant temperature, mass density ρ and kinematic viscosity ν. Moreover, only two-dimensional cross sections are considered. As a consequence of constant density the continuity equation

$$\nabla \cdot \mathbf{u} = 0 \tag{1}$$

must hold, where u denotes the velocity field with non-zero components only in the cross section plane. By introducing the vorticity

$$\omega = \nabla \times \mathbf{u} \tag{2}$$

which is only a scalar value by virtue of the previous, the Navier-Stokes equations can be simplified to yield the so-called vorticity transport equation (VTE)

$$\frac{\partial \omega}{\partial t} + (\mathbf{u} \cdot \nabla)\omega = \nu \nabla^2 \mathbf{u}\,. \tag{3}$$

If a solution for (3) is searched, a closing relation which allows for reconstructing the velocity for a given vorticity field is needed which is given by the Biot-Savart integral for a given onset flow $\mathbf{U}_\infty$:

$$\mathbf{u}(\mathbf{x}) = \mathbf{U}_\infty - \frac{1}{2\pi} \int \frac{\omega(\mathbf{x}') \times (\mathbf{x}' - \mathbf{x})}{|\mathbf{x}' - \mathbf{x}|^2}\, \mathrm{d}\mathbf{x}'\,. \tag{4}$$

In this paper the main focus for solving (3) is put on Discrete Vortex Methods (DVMs), which is based on a representation of the vorticity field $\omega(\mathbf{x})$ by a large number of vortex particles of a given size σ according to

$$\omega(\mathbf{x}) = \sum_i \delta_\sigma(\mathbf{x} - \mathbf{x}_i)\Gamma_i \tag{5}$$

where Γ_i is the total circulation of the vortex particle and the core function δ_σ describes the shape of the vortex. Commonly the core function is a Dirac delta like function like a Gaussian distribution. Contrary to finite difference of element methods, where the vorticty is considered at fixed grid points, the position of the vortex particles moves with the fluids velocity field i.e. the problem is considered in a body-fixed coordinate system in a Lagrangian manner. A typical instantaneous plot of the vortex particle positions is indicated in Figure 1.

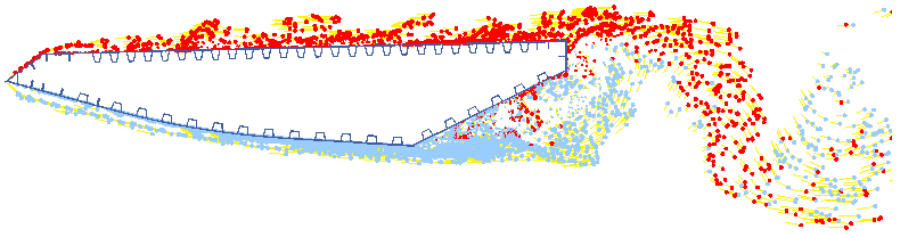

FIGURE 1 - TYPICAL FLOW PATTERN OF VORTEX PARTICLES AROUND CROSS SECTION

This approach simplifies significantly the treatment of boundary conditions along the cross section outline. It has been pointed out by Walther and Larsen [1997] that it is sufficient to demand the no-penetration boundary condition with zero normal components together with conservation of total circulation, because then the no-slip condition with vanishing tangential

components is fulfilled automatically. The boundary is modeled by introducing a surface vorticity layer determined by boundary element or Martensen method [Lewis, 1991].

Due to the ansatz (5) the Biot-Savart integral can be evaluated as sum leading to N sums with (N-1) terms for the N vortex particles. This is a well known problem in many body physics which is also encountered e.g. in electrodynamics and astrophysics. Carrier et al. [1988] devised the so-called adaptive multipole algorithm (AMA) which is nowadays the most widely used for such problems. Consequently is also the method of choice for the present implementation. Other methods which are linked to $N \times N$ particle interactions also used in bluff aerodynamics are lumping and cell-to-cell methods [Spalart, 1988] and the P^3M method [Morgenthal, 2002].

The numerical integration of the vorticity transport equation is performed by using a fractional step method. First, convection (second term on left hand side of VTE) is treated with a forward Euler or explicit Adams-Bashforth schemes. The diffusion term on the right hand side is treated with the random walk method suggested by Chorin [1973]. Each particle is moved a randomly distributed distance into a random direction. For large numbers of particles this approach converges to the exact solution of the diffusion operator. Simultaneously to the diffusion of free vortices the vorticity bound in the layer next to the body outline is converted into nascent vortices and diffused into the flow. The vorticity-flux created by the nascent vortices is also used to determine the time-dependent pressure distribution along the cross section outline up to an unknown datum value. By integrating the pressure along the surface time histories $D(t)$ of drag and $L(t)$ of lift force as well as $M(t)$ for overturning moment can be obtained. The directions of forces are defined in Figure 2, where the onset flow is expressed by its absolute value U_∞ and direction α.

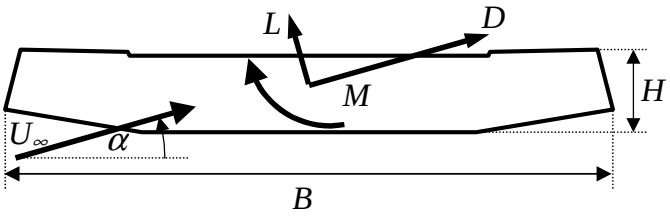

FIGURE 2 - DEFINITION OF AERODYNAMIC FORCES AND WIND DIRECTION

POST-PROCESSING OF TIME HISTORIES

To compare the aerodynamic performance of different cross sections and to scale wind tunnel models it is usual to relate all velocities to the onset velocity U_∞ and lengths to a typical length scale ℓ. The Reynolds number

$$\mathrm{Re} = \frac{u_\infty b}{\nu} \tag{6}$$

gives the ratio of inertial to viscous forces. Therefore the flow situation around a model and the full scale cross section equivalent if they are considered at the same Reynolds number, a necessary requirement to perform wind tunnel tests. However it must be noted that admissible Reynolds numbers in wind tunnels are of order 10^5, while in reality $\mathrm{Re} > 10^7$. Consequently an important preliminary for such tests is that the flow around bluff bodies like bridge deck sections is quite independent of the Reynolds number. This is in general justified by arguing that there are clearly defined vortex separation points at the outline corners, which remain the same for all

velocities .

From the time histories calculated by the CFD algorithm, time averaged forces and moments can be obtained. In non dimensional form they are related to the dynamic pressure ½ ρU_∞^2 to yield the steady state coefficients for fixed cross sections:

$$C_D = \frac{D}{\frac{1}{2}\rho U_\infty^2 \ell_D} \qquad C_L = \frac{L}{\frac{1}{2}\rho U_\infty^2 \ell_L} \qquad C_M = \frac{M}{\frac{1}{2}\rho U_\infty^2 A}, \tag{7}$$

where ℓ_D and ℓ_L are suitable normalization lengths for drag and lift and A the normalization area for moment. In bridge engineering it is common to relate the normalization for lift and moment to the width B of the cross section: $\ell_L = B$ and $A = B^2$ and the drag to the height H. In the above equations it should be noted that the forces are given per meter of span length. Since the dependence on wind velocity has been neglected, the coefficients are only dependent on wind direction α.

In the field of aeronautics the Theodorsen theory [1935] states that the aerodynamic forces on a moving cross section are linear in the deflections and their first two derivatives. For bluff aerodynamics the time dependent lift and moment forces are expressed by the so called flutter derivatives H_i^* and A_i^* as suggested by Simiu and Scanlan [1996]. They relate the resulting forces for vertical and torsional displacements h and α, and their first derivatives with respect to time:

$$\begin{aligned} L &= \tfrac{1}{2}\rho U_\infty^2 \ell_L \left(KH_1^* \frac{\dot{h}}{U_\infty} + KH_2^* \frac{B\dot{\alpha}}{U_\infty} + K^2 H_3^* \alpha + K^2 H_4^* \frac{h}{B} \right) \\ M &= \tfrac{1}{2}\rho U_\infty^2 A \left(KA_1^* \frac{\dot{h}}{U_\infty} + KA_2^* \frac{B\dot{\alpha}}{U_\infty} + K^2 A_3^* \alpha + K^2 A_4^* \frac{h}{B} \right) \end{aligned} \tag{8}$$

The flutter derivatives are dependent on reduced frequency $K = B\omega / U_\infty$ where ω is the circular frequency of oscillation. It should be noted that due to historical reasons in compatibility to Theodorsen the quantities are given with inverse sign compared to the steady state coefficients, e.g. with positive sign of lift and heave in downward direction. In most practical cases the flutter derivatives are not given in dependence of K, but of the reduced velocity $U_{red} = 2\pi / K$.

To calculate the flutter derivatives, the cross section is considered for forced pure vertical or torsional oscillation at different values of reduced velocity [Larsen and Walther, 1998]. By arguing that the driving forces for oscillation of given frequency must also be harmonic but phase shifted, a suitable ansatz can be inserted into (8) to obtain the desired coefficients. A vertical oscillation yields the coefficients H_1^*, H_4^*, A_1^* and A_4^*. The other coefficients are calculated by assuming torsional oscillations.

Application to Stonecutters Bridge

The application of CFD analysis is presented by considering the twin girder deck of the Stonecutters Bridge in Hong Kong (Project Engineers: Ove-Arup, Hong-Kong). A detailed presentation of one girder is illustrated in Figure 1, the twin girder system is outlined in Figure 3. The bridge is a cable-stayed bridge with a main span of 1018m, side spans of 298m, and a towers height of 290m. The deck to the main span is a twin girder steel deck, whilst the side spans are of concrete, which are to be built in advance of cable stay erection to counterbalance and stabilize the slender light-weighted main span deck.

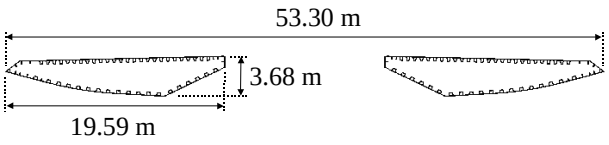

FIGURE 3 - TWIN GIRDER SYSTEM OF STONECUTTERS BRIDGE

A CFD calculation was performed for the deck, where a rigid connection between the twin girders are assumed. The total width of 53.3 m was chosen as normalization length for all coefficients. Good agreement was found with results obtained with DVMFLOW (cf. Larsen and Walther [1998]). The results are shown in Figure 4.

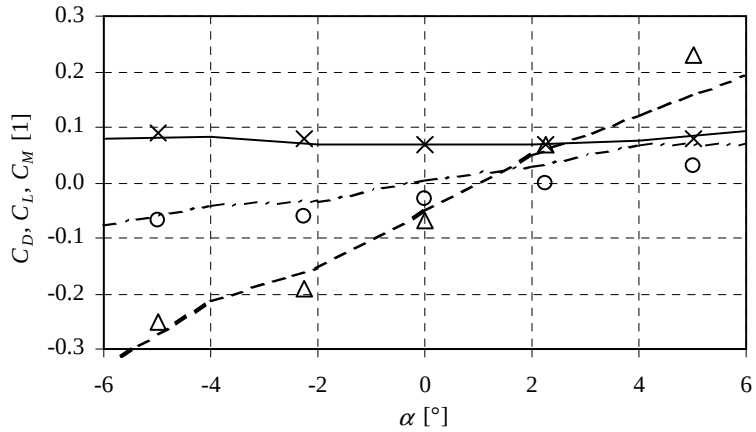

FIGURE 4 - STEADY STATE COEFFICIENTS C_D (SOLID LINE, X), C_L (DASHED LINE, O) AND C_M (DASH-DOTTED LINE, Δ) FOR STONECUTTERS BRIDGE, RESULTS MARKED WITH SYMBOLS ARE DVMFLOW RESULTS

Further successfull application of the implemented CFD code was reported in [Beier et al., 2007] and [Stampler at al., 2007].

Application to Storebælt Bridge

Flutter investigations were performed for the Great Belt East bridge. The main cross section is a hollow box steel girder a width of 32 m and a height of 4.3 m. The flutter derivatives calculated with the implemented DVM for Re = 10^5 are shown in Figue 5 for the vertical coefficients H_i^* and in Figure 6 for the torsional coefficients A_i^*. A good agreement with numerical results obtained by Walther [1994] is observed.

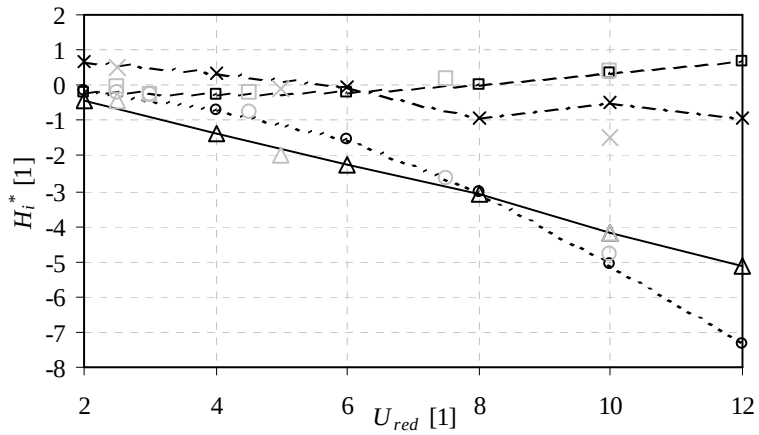

FIGURE 5 - FLUTTER DERIVATIVES H_1^* (Δ), H_2^* (□), H_3^* (O) AND H_4^* (X) OF GREAT BELT BRIDGE. RESULTS BY WALTHER [1994] ARE INDICATED BY LIGHT SYMBOLS.

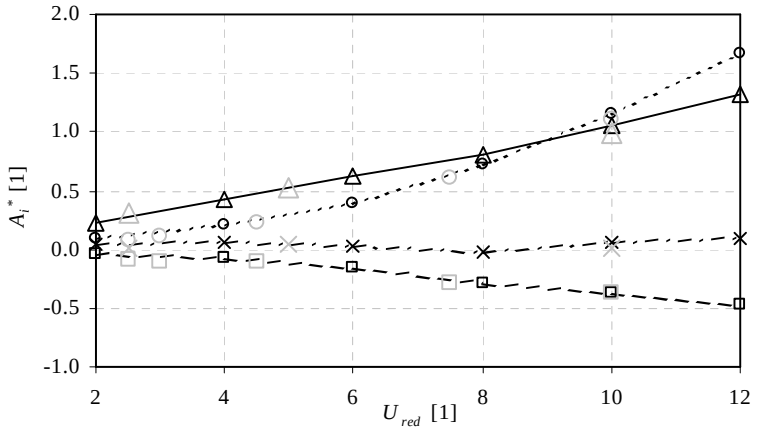

FIGURE 6 - FLUTTER DERIVATIVES A_1^* (Δ), A_2^* (□), A_3^* (O) AND A_4^* (X) OF GREAT BELT BRIDGE. RESULTS BY WALTHER [1994] ARE INDICATED BY LIGHT SYMBOLS.

WIND BUFFETING ANALYSIS

The wind buffeting analysis takes into account that the relative flow velocity is not constant for two reasons. First, the wind direction is not uniform in time, but distributed stochastically. This fact is modeled by introducing time dependent zero mean additional velocities *u* in along and *w* in transverse wind direction. And second, the velocity of the structure adds to the relative velocity, leading to an overall wind velocity U_{eff} with direction α_{eff} as indicated in Figure 7.

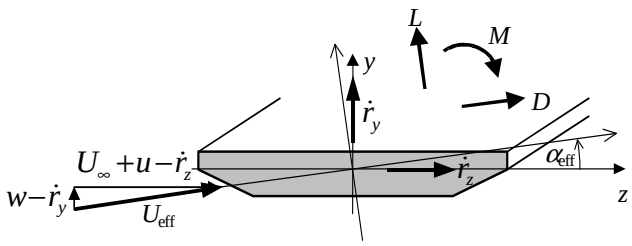

FIGURE 7 - CONTRIBUTIONS TO EFFECTIVE VELOCITY FOR BUFFETING ANALYSIS

For the further analysis it is assumed that the forces are still described by the steady state coefficients (i.e. only small deviation of undisturbed case). Consequently only a small twist ϑ_x can be expected an a linear approximation $C_x(\alpha_{\text{eff}}) = C_x(0) + \alpha_{\text{eff}}\ C_x'(0)$ holds. If these approaches are used in (7) and squares of the additional small velocities are neglected, the following relation for the aerodynamic forces hold:

$$\begin{pmatrix} D \\ L \\ M \end{pmatrix} = \frac{1}{2}\rho U_\infty^2 \begin{pmatrix} \ell_D C_D \\ \ell_L C_L \\ A C_M \end{pmatrix}_{\text{st}} + \rho U_\infty \begin{pmatrix} \ell_D C_D u + \frac{1}{2}(\ell_D C_D' - \ell_L C_L) w \\ \ell_L C_L u + \frac{1}{2}(\ell_L C_L' + \ell_D C_D) w \\ A C_M u + \frac{1}{2} A C_M' w \end{pmatrix}_{\text{dyn}} - \rho U_\infty \begin{pmatrix} \ell_D C_D \dot{r}_z + \frac{1}{2}(\ell_D C_D' - \ell_L C_L) \dot{r}_y \\ \ell_L C_L \dot{r}_z + \frac{1}{2}(\ell_L C_L' + \ell_D C_D) \dot{r}_y \\ A C_M \dot{r}_z + \frac{1}{2} A C_M' \dot{r}_y \end{pmatrix}_{\text{damp}} + \rho U_\infty \begin{pmatrix} \frac{1}{2}\ell_D C_D' \vartheta_x \\ \frac{1}{2}\ell_L C_L' \vartheta_x \\ \frac{1}{2} A C_M' \vartheta_x \end{pmatrix}_{\text{stiff}} \tag{9}$$

In (9) different contributions are classified: the static (st) and dynamic (dyn) loads are terated as addizional loads, while the structural elements are modified with additional damping (damp) and stiffness (stiff) terms. The next step is to consider the resulting system in modal space, based on the eigenforms of the structure in still air.

By providing additional information about the local wind velocity distribution, turbulence, power spectral density and coherence, in the following summarized as “wind profile” (see Janjic and Pircher [2004]), the peak factors of the displacement and internal forces can be estimated. To this end a multimode response calculation with modified mechanical admittace due to the additional stiffness and damping in (9) is performed in frequency space.

Application to Stonecutters Bridge

A detailed wind buffeting analysis was perfomed for the Stonecutters bridge. To obtain as accurate wind profile information, a 50 m high mast was constructed to measure wind speed an direction. Thus a detailed stochastic description of the local wind was available for the computer aided buffeting analysis. The distribution of different calculated internal forces is shown in Figure 8.

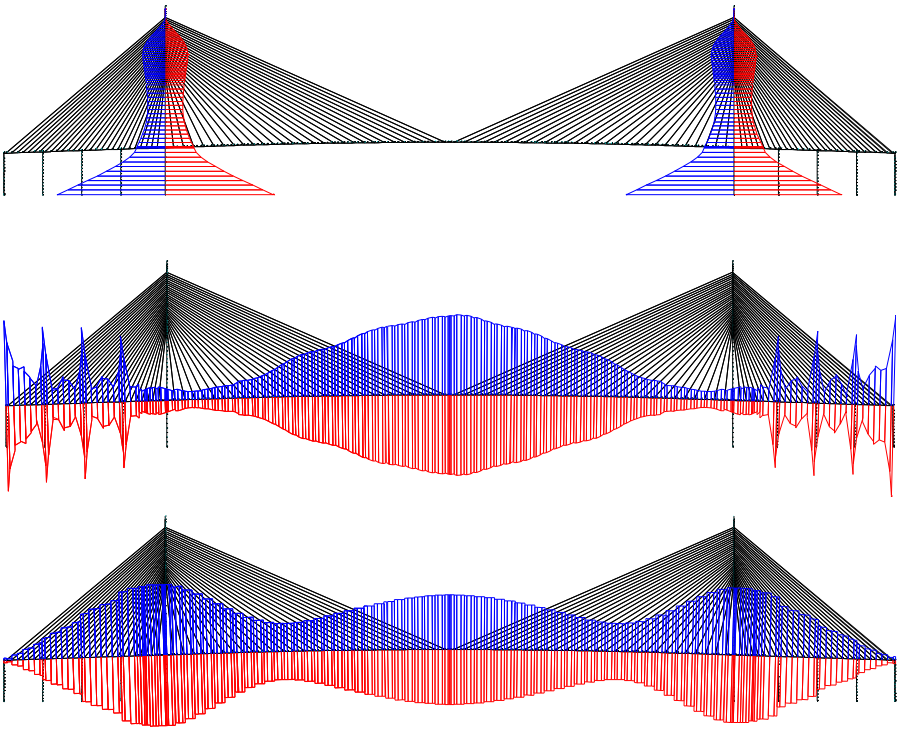

FIGURE 8 - TOWER BENDING MOMENT (TOP), DECK BENDING MOMENT (MIDDLE) AND DECK NORMAL FORCE OBTAINED BY A WIND BUFFETING ANALYSIS OF THE STONECUTTERS BRIDE

ADDITIONAL WIND DESIGN CHECKS

Galloping instability

Across wind galloping is a low-frequency vertical oscillation. If the resulting vertical force is evaluated based on the steady state coefficients, the derivative of the lift coefficient with respect to the attack angle can be identified as additional damping term in the equations of motion. Depending on its sign either damped or sustained oscillations are possible. A necessary criterion for sustained oscillation is the so-called Glauert-Den Hartog criterion

$$\left(C'_{L0} + \frac{\ell_d}{\ell_l} C_{D0} \right) < 0 \tag{10}$$

Since the slope of the lift coefficient is always positive for the Stonecutters bridge, galloping is not expected to occur.

Torsional divergence

Torsional divergence occurs, if a small increase of twist of the deck results in an additional twisting moment which can not be counterbalanced by the torsional stiffness of the deck. Since the additional moment depends on the wind velocity, a critical velocity can be found which must not be excessed to guarantee stability of the deck. It is given by

$$U_{c,\mathrm{div}} = \sqrt{\frac{2k_\alpha}{\rho A C'_{M0}}} \tag{11}$$

where k_α is the torsional stiffness, which is normaly expressed by the lowest torsional circular eigenfrequency ω_α and moment of inertia I via $k_\alpha = I\ \omega_\alpha$.

For the lowest torsional mode during construction state at f = 0.429 Hz a critical wind speed of Uc,div = 173 m/s was calculated for the Stonecutters bridge.

Classical flutter

The term classical flutter refers to a flow driven coupled two-degree-of-freedom oscillation of the cross section. To solve the flutter problem, a coupled system of equations of motion is constituted where the forces are given by (8). The critical velocity is the point of transition from damped oscillation to sustained oscillation. If the solutions are denoted in complex form, the according circular frequency at the critical velocity must be a real number and a solution can be obtained following Simiu and Scanlan [1996]. By inserting the ansatz $(h, \alpha) = (h_0, \alpha_0) \exp(\omega t)$ into the equations of motion a linear system $\mathbf{M}\cdot(h_0, \alpha_0) = 0$ is obtained. This system has non-trivial solutions only if the determinant of the coefficient matrix vanishes. Because of the used ansatz, the matrix coefficients are complex numbers and the determinant evaluates to a polynomial of fourth order in ω. By considering the real and imaginary part of this equation separately, which is possible because the frequency is real, two real polynomials of fourth and third order are established. The coefficients of these polynomials depend on K via the involved flutter derivatives, and a common solution to both polynomials to fulfill $\det(\mathbf{M}) = 0$ is only possible for certain values of the reduced frequency K. Once such values for the reduced frequency K_{crit} and frequency ω_{crit} have been found, the critical velocity can be calculated from the definition of the reduced frequency.

The evaluation of the flutter derivatives for the Great belt bridge yields a critical flutter velocity of 41.8 m/s, compared to wind tunnel measurements of 37.6 m/s [Reinhold et al. 1992].

Torsional flutter

For certain types of cross sections the flutter coefficient A_2^* becomes positive. In this case unstable solutions to the flutter equations are possible even if no coupling occurs, because the term incluiding A_2^* leads to additional damping so that the total damping can be zero or negative. By inspecting Figure 6 it can be seen that the deck of the Great Belt bridge is not susceptible to torsional flutter.

CONCLUSIONS

This paper outlined the theoretical background of the necessary steps of wind design of long span bridges. To this end the overall process was spitted into the characterisation of the air flow and corresponding aerodynamic coefficients by means of the DVM. The second step was to evaluate the different design checks with the previously calculated coefficients. Several tests for the steady state coefficients predicted a good applicability for the full scale model. Comparisons of the flutter prognosis with wind tunnel test as well as numerical simulations showed a good agreement.

The overall analysis was performed within one software package. The advantage of this approach was that the same cross sections can be used as basis for the structural analysis and the CFD calculation. Moreover, the data exchange between different analysis tasks was simplified

and accelerated. Thus the application of such an all-in-one solution significantly improves the efficiency of design tools for long span bridges.

REFERENCES

[1] Beier, M, Loredo Souza, A, M, Rocha, M, M, Janjic, D, Domaingo, A, "Wind Tunnel Validation of Vortex Method for Aerodynamic Coefficients", *Proc. IABSE-Symposium*, Weimar, 2007.

[2] Carrier, J, Greengard, L, and Rokhlin, V, "A Fast Adaptive Multipole Algorithm for Particle Simulations", *SIAM J. Sci. Stat. Comput.*, 9**,** 1988, 669-686.

[3] Chorin, A, J, "Numerical study of slightly viscous flow", *J. Fluid Mech.*, 57, 1973, 785-795.

[4] Janjic, D, and Pircher, H, "Consistent Numerical Model for Wind Buffeting Analysis of Long-Span Bridges", *Proc. IABSE-Symposium*, Shanghai, 2004.

[5] Larsen, A, and Walther, J, H, "Discrete vortex simulation of flow around five generic bridge deck sections", *J. Wind Eng. Ind. Aerodyn*., 77 & 78, 1998, 591-602.

[6] Lewis, R, I, *Vortex element methods for fluid dynamic analysis of engineering systems*, Cambridge University Press, Cambridge, 1991.

[7] Morgenthal, G, *Aerodynamic Analysis of Structures Using High-resolution Vortex Particle Methods*, PhD Thesis, University of Cambridge, Cambridge, 2002.

[8] Reinhold, T, A, Brinch, M, and Damsgaard, A, "Wind tunnel tests for the Great Belt Link". *Proc. First International Symposium on Aerodynamics of Large Bridges*, 1992, 255-267.

[9] Simiu, E, and Scanlan, R, H, *Wind Effects on Structures*, third edition, John Wiley & Sons, New York, 1996.

[10] Spalart, P, R, "Vortex Methods for Separated Flows", *NASA Technical Memorandum*, 100068, 1988.

[11] Stampler, J, Janjic, D, Domaingo, A, "Integrated Computer Wind Design for Bridge Engineering", *Proc. IABSE-Symposium*, Weimar, 2007.

[12] Strømmen, E, N, *Theory of Bridge Aerodynamics*, Springer Verlag, Berlin Heidelberg, 2006.

[13] Theodorsen, T, „General Theory of Aerodynamic Instability and the Mechanism of Flutter", *NACA Report*, 496, 1995.

[14] Walther, J, H, *Discrete Vortex Method for Two-Dimensional Flow past Bodies of Arbitrary Shape Undergoing Prescribed Rotary and Translational Motion*, PhD Thesis, Technical University of Denmark, Lyngby, 1994.

[15] Walther, J, H, and Larsen, A, "Two dimensional discrete vortex method for application to bluff body aerodynamics", *J. Wind Eng. Ind. Aerodyn*., 67 & 68, 1997, 183-193.